Available online at www.sciencedirect.com

ScienceDirect

IFAC PapersOnline CONFERENCE PAPER ARCHIVE

IFAC PapersOnLine 51-18 (2018) 530–535

Model Predictive Control of Simulated Moving Bed Chromatography for Binary and Pseudo-binary Separations: Simulation Study

Ju Weon Lee*. Andreas Seidel-Morgenstern**

**Max-Planck-Institute for Dynamics of Complex Technical Systems, Magdeburg, Germany (Tel: +49 391-6110392; e-mail: lee@mpi-magdeburg.mpg.de).*
***Max-Planck-Institute for Dynamics of Complex Technical Systems, Magdeburg, Germany (e-mail: seidel-morgenstern@mpi-magdeburg.mpg.de).*
***Institute of Process Engineering, Otto von Guericke University, Magdeburg, Germany (e-mail: anseidel@ovgu.de).*

Abstract: Simulated moving bed (SMB) processes have been applied to petrochemical, pharmaceutical, and fine chemical industries to separate products in high purity and yield since it was introduced in 1960s. Owing to process complexity and operational sensitivity, the control and dynamic optimization of the SMB process are still challenging issues. In this work, a simplified process model with linear isotherms was introduced to estimate process states of conventional four-zone SMB chromatography. In a simulation study, a controller can estimate current process states and find the optimal operating conditions 'switch by switch' up to moderately nonlinear ranges of the competitive Langmuir isotherms. Furthermore, the controller works for the process with system void volumes and delayed feedback information.

Keywords: Model Predictive Control, Simulated Moving Bed, Linear Isotherms, Delayed Feedback

1. INTRODUCTION

A Simulated moving bed (SMB) process, a continuous chromatographic separation process using simulated counter-current movements of the solid and liquid phases, was introduced in 1960s (Broughton, D.B. et. al. 1970). The conventional SMB process consists of several packed bed columns forming a ring that is divided into four zones by two inlets (*feed* and *desorbent*) and two outlets (*extract* and *raffinate*) as shown in Fig. 1.

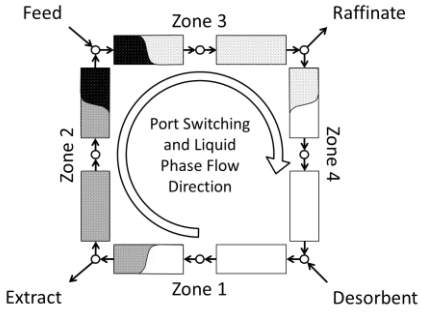

Fig. 1. Schematic illustration of the conventional four-zone SMB process.

The ports are shifted to the same direction of the liquid phase flow to simulate counter-current flow of the solid phase. Through the *feed* port, a feed mixture is fed into the process continuously. The mixture components are separated in the chromatographic columns and collected at two outlets (*raffinate*: less retained components, *extract*: more retained components). To manipulate the zone flow-rates individually, one more inlet called *desorbent* is located in between the zones 1 and 4. Because of the periodic repetition of port switching, the SMB process does not reach the steady-state, but 'cyclic steady-state'

Over the past few decades, many researchers applied the empirical and model based controllers to the conventional four-zone SMB processes to control product quality and to optimize process performance. As shown in Fig. 1, the four-zone SMB needs to be decided four operation parameters with one fixed condition (normally, the feed flow-rate or the port switching interval). A multi-PID controller for MIMO system was applied to control two product stream purities with the foot print of the internal profiles observed with the UV detectors (Schramm, H. et. al. 2003). A repetitive MPC was also applied to reject periodic disturbance of the SMB process (Natarajan, S. et. al. 2000), and a multi-MPC with the wave theory was introduced for the nonlinear SMB process (Vilas, C. et. al. 2011). An NMPC with a rigorous process model was also applied in three zone RSMB process to produce high fructose corn syrup (Toumi A. et. al. 2004 and 2007). Application of the Karman filter to the SMB process and its experimental validation using the observation of both online UV detector signals and HPLC analysis were reported (Grossmann, C. et. al. 2010a, b). A prediction-correction method with a rigorous chromatographic column model was proposed to optimize the SMB process with NLP solver (Bentley J. et. al 2013).

A rigorous SMB process model is a PDE system with competitive nonlinear adsorptions. Therefore, a lot of information that is not easy to be obtained in a real case is required. For example, Toumi et. al. observed the internal concentration profiles, which requires lots of analysis efforts in each port switching internal, to determine the process

10.1016/j.ifacol.2018.09.370

parameters. In this work, a novel simplified process model that mimics the four-zone SMB process with known process outputs was applied to estimate the process parameters and to predict the optimal operating conditions. Both binary and pseudo-binary separation cases were considered.

2. PROCESS DESCRIPTION

2.1 Configuration of Four-Zone SMB

Fig. 2 shows the considered four-zone SMB configuration. Due to structural complexity, a SMB process includes a lot of system void volumes (described as a continuously stirred tank, CST in Fig. 2).

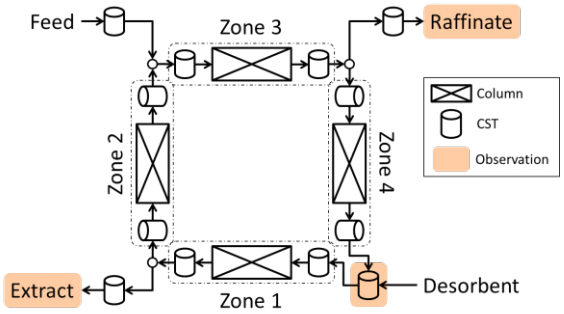

Fig. 2. Schematic illustration of the four-zone SMB configuration with one column per zone.

The simplest configuration, one column per zone including the system void volumes as shown in Table 1 was chosen. Assuming that all system void volumes are considered as a CST, feeding of the feed mixture and collection of outlet products are delayed by three external void volumes (V_{Feed}, V_{Extr}, and V_{Raff}). To collect a sample at the *desorbent* port, one mixer is connected in between the zones 1 and 4 (V_{Rcyl}). Inside of the SMB ring, two CSTs are connected before and after each column (V_{CF} and V_{CR}).

Table 1. Considered SMB configurations with system void volumes.

# of columns	1-1-1-1
Void volumes	
Internal (in SMB ring)	before/after column (V_{CF}, V_{CR}) mixer at desorbent port (V_{Rcyl})
External (out of SMB ring)	feed inlet to SMB ring (V_{Feed}) SMB ring to extract outlet (V_{Extr}) SMB ring to raffinate outlet (V_{Raff})

In real case, a certain time is required to collect and analyze the component concentrations in the observation ports, so that all operations were performed with the fixed switching interval. At the fixed switching interval, the four-zone SMB process has four design parameters, so that all operating conditions can be determined from four zone flow-rates (Q_1 to Q_4).

2.2 Collectable Information of the SMB process

To consider an experimentally feasible observation of the SMB process, the component concentrations at two outlets (c_{Extr} and c_{Raff}) and the CST at the *desorbent* port (c_{Rcyl}) were collected. Assuming that all collected samples are well mixed and collected in one switching interval, the average outlet concentrations and the desorbent port concentrations can be obtained. If a proper analysis method is fast enough to analyze all samples in one switching interval, it is possible to obtain all information with one switching interval delay. Otherwise, more delayed or sparser information can be obtained in each switching interval. Table 2 shows the considered delay scenarios.

Table 2. Considered delay and feedback information scenarios for the controller.

Delayed switches	0 (No delay), 1, 2, 4
Information	Full (all of c_{Extr}, c_{Raff}, and c_{Rcyl}) Single (one of c_{Extr}, c_{Raff}, and c_{Rcyl})

Single information means that the concentration data in one stream can be obtained in each switching interval. The analysis order is $c_{Raff} \rightarrow c_{Extr} \rightarrow c_{Rcyl} \rightarrow c_{Raff}$.

3. PREDICTIVE CONTROL

3.1 Simplified Process Model with Linear Isotherms

A simplified process model that can simulate an SMB process was developed to estimate the process parameters and calculate state variables.

In chromatographic column, the migration of the concentration profiles can be described in two phenomena, the penetration along with the liquid phase flow and the dispersion by concentration gradient. In rigorous numerical methods, time and space domains are divided into fine meshes and the discretized PDEs are solved in each mesh. Therefore, it takes enormously long time to simulate the SMB process.

Fig. 3 shows the typical internal concentration profiles of the 4-zone SMB process. In well-designed operating conditions, desorption and adsorption take place in the zones 1 and 2, and in the zones 3 and 4, respectively. Therefore, two different linear isotherms for desorption and adsorption waves were applied. The migration velocity of the component i is,

$$v_i = \frac{Q}{1+k_i} \tag{1}$$

where v_i is the volumetric migration velocity of the component i, Q is the volumetric flow-rate of the liquid phase, and k_i is the retention factor of the component i. After migrating the concentration profiles with the given velocities, the migrated concentration profiles are divided with the given cell volume (δ), and then distributed with the average cell concentrations as below.

$$c_{i,j}^{f} = \frac{\int_{\delta_j} c_i\, dV + \int_{\delta_{j-1}} c_i\, dV}{\delta_j + \delta_{j-1}},\ c_{i,j}^{r} = c_{i,j-1}^{f}, j = 1,2,\dots,N_\delta \tag{2}$$

where c^f and c^r are the concentrations of component at the front and rear ends of the cell volume after updating cell distribution, respectively. Knowing the initial internal concentration profiles at a certain switching interval (e.g. zero concentrations at the beginning of the SMB process), the initial internal concentration profiles at the next switching interval and the average concentrations of each port can be

calculated. For one component, this simplified process model requires four parameters, k_{Des}, k_{Ads}, δ_{Des}, and δ_{Ads}. Subscripts *Ads* and *Des* denote desorption and adsorption, respectively.

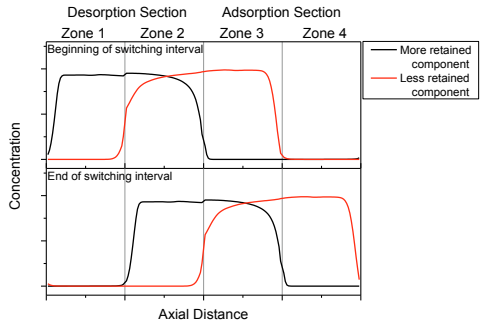

Fig. 3. Typical internal concentration profiles of the four-zone SMB process with well-posed operating conditions.

3.2 Parameter Estimation

To estimate four parameters for each component (k_{Des}, k_{Ads}, δ_{Des}, and δ_{Ads}), a gradient-based optimization method needs additional process simulation to calculate derivatives and matrix calculation that are difficult to be implemented in parallel computation. Therefore, in this work, the parallelized Nelder-Mead simplex method (Lee, D. et. al. 2007) was used to minimize the following objective function.

$$G_i(k_{Ads}, \delta_{Ads}, k_{Des}, \delta_{Des}) = \sum_{m=SC_C-SC_D}^{SC_C-SC_D-SC_O} \sum_{l=1}^{L} w_l \left| \log\left\{ \frac{\max(c^*_{i,l,m}, \alpha)}{\max(c_{i,l,m}, \alpha)} \right\} \right| \quad (3)$$

where c and c^* are the calculated and observed average concentrations, L is the number of observed ports, SC is the switching count, the subscripts C, D, and O denote the current, delayed, and the observed switch counts, respectively, w is the weight factor, and α is a small number (α = 1e-9 g/L). All weight factors fixed to 1. If the observed and calculated concentrations are smaller than α, the logarithm term of the objective function becomes zero, so that α represents the minimum concentration that can be observed by a proper analysis method. Concentration data at the observation ports were used to estimate the parameters.

3.3 Control Strategy

Each zone in the four-zone SMB process has a distinct role. In the zones 1 and 4, the packed solid and the liquid phases are respectively regenerated to prevent contamination of outlet streams by recycled impurities. In the zones 2 and 3, the feed mixture is split into two parts, more retained component(s) and less retained component(s). Therefore, the zone flow-rates can be coupled in two groups, Q_2-Q_3 and Q_1-Q_4 for the fast screening of the optimal operating conditions.

Since the parallelized Nelder-Mead method was also used for the screening, good initial conditions that can lead to good local optimum point is needed. As described in the 'triangle theory' (Storti, G. et. al. 1993) the estimated retention factors can give good initial conditions as follows.

$$Q_1 = \varepsilon V_C(1 + k_{A1})/t_S, Q_2 = \varepsilon V_C(1 + k_{B1})/t_S$$

$$Q_3 = \varepsilon V_C(1 + k_{A2})/t_S, Q_4 = \varepsilon V_C(1 + k_{B2})/t_S \quad (4)$$

where ε is the void fraction of the column, V_C is the empty column volume, t_S is the port switching interval, the subscripts $A1$ and $A2$ represent the most and the least retained components in the desired extract products, respectively, and the subscripts $B1$ and $B2$ represent the most and the least retained components in the desired raffinate products, respectively ($A1 = A2$ and $B1 = B2$ in binary separations).

For the optimization of the zones 1 and 4, the following cost function was used.

$$J_{14} = \left(\frac{C_{T,Rcyl} - \sum_{i=1}^{N_T} c_{i,Rcyl,SC_C+SC_F}}{C_{T,Rcyl}} \right)^2 + \left(\frac{C_{W,Rcyl} - \sum_{i=1}^{N_W} c_{i,Rcyl,SC_C+SC_F}}{C_{W,Rcyl}} \right)^2 \quad (5)$$

where C_{Rcyl} is the set value of c_{Rcyl}, N is the number of components, the subscripts T and W denote the target and the waste components, respectively, and the subscript F denotes the predicted future switch counts, respectively. For the complete regeneration of the solid and the liquid phases in the zones 1 and 4, $C_{T,Rcyl}$ and $C_{W,Rcyl}$ were set to one-thousandth of the feed concentrations.

After screening the optimized flow-rates for the zones 1 and 4, the following cost function was used for the screening of the zone 2 and 3 flow rates.

$$J_{23} = \left(P - p_{SC_C+SC_F}\right)^2 + \left(Y - y_{SC_C+SC_F}\right)^2$$

$$p_{SC_C+SC_F} = \frac{\sum_{i=1}^{N_T} c_{i,TS,SC_C+SC_F}}{\sum_{i=1}^{N} c_{i,TS,SC_C+SC_F}}$$

$$y_{SC_C+SC_F} = \frac{\sum_{i=1}^{N_T} Q_{TS} c_{i,TS,SC_C+SC_F}}{\sum_{i=1}^{N_T} Q_{TS} c_{i,TS,SC_C+SC_F} + \sum_{i=1}^{N_T} Q_{WS} c_{i,WS,SC_C+SC_F}} \quad (6)$$

where P and Y are respectively the set purity and yield of the target component, p and y are respectively the purity and yield of the target component, and the subscripts *TS* and *WS* denote the target and waste streams, respectively. If the target stream is the extract stream, the waste stream is the raffinate stream, and vice versa. The future switching count, SC_F was fixed to 4, and the constant future operating conditions were used.

The controller routines were coded with Microsoft Visual C++ (Microsoft Inc., Ver. 2015 Express Edition). Fig. 4 shows the proposed feedback control flow diagram.

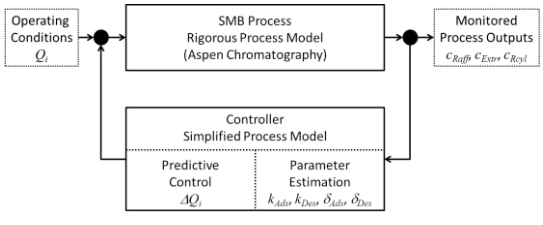

Fig. 4. Flow diagram of the proposed feedback control with simplified process model.

3.3 Rigorous SMB Process Simulation

To validate the proposed controller, a commercial rigorous SMB simulator, Aspen Chromatography (Aspen Technology

Inc., Ver. 7.1) was used to mimic the SMB process. The mass-balance equation for the chromatographic column with the competitive Langmuir isotherm is,

$$v_L \frac{\partial c_i}{\partial z} + \varepsilon \frac{\partial c_i}{\partial t} + (1-\varepsilon)\frac{\partial q_i}{\partial t} = \varepsilon D_L \frac{\partial^2 c_i}{\partial z^2}$$
$$\frac{\partial q_i}{\partial t} = k_{eff,i}(q_i^* - q_i)$$
$$q_i^* = q_{Max}\frac{K_i c_i}{1+\sum_{j=1}^{N} K_j c_j} \quad (7)$$

where v_L is the linear velocity of the liquid phase, D_L is the axial dispersion coefficient, q_i and q^*_i are the concentration of component i in the solid phase and the solid film, k_{eff} is the lumped mass transfer coefficient, and q_{Max} and K are the Langmuir isotherm parameters. The Chung and Wen correlation (Chung, C.F. et. al. 1968) was used to estimate the axial dispersion coefficient. The parameters used in the rigorous simulation are listed in Table 3.

Table 3. Parameters for the "Aspen Chromatography" simulation.

Column	10 cm (length), 1.0 cm (i.d.), ε =0.7
Solid phase	5 μm (particle radius), 1.0 (shape factor)
Liquid phase	0.948 g/cm^3 (density), 2.55 cP (viscosity)
Parameters	
k_{eff} [1/min]	A: 1000, B: 1000, C: 1000
q_{Max}	1167 g/L
K [L/g]	A: 0.018, B: 0.01, C: 0.006

To communicate data between the controller and the rigorous process simulator, windows shell scripting with VBScript was used. For the binary separation, components A and B were considered.

4. RESULTS AND DISCUSSION

4.1 Simplified Process Model for Four-Zone SMB

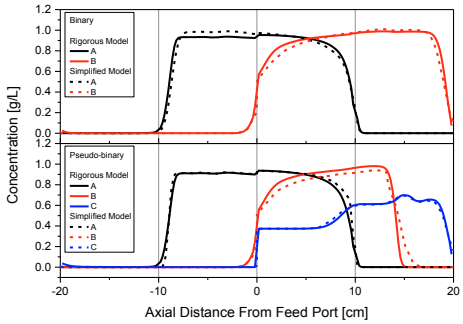

Fig. 5. Comparisons of the internal concentration profiles calculated by the rigorous model and the simplified model at the end of port switching interval in cyclic steady-state (upper: binary separation case, lower: pseudo-binary separation case, c_{Feed} = 1.0 g/L each, the target: component A in the extract stream).

Assuming that all columns in the SMB process are clean at the beginning, the controller can estimate the concentration profiles at the end of port switching interval. From the concentration profiles at the beginning and end of port switching interval, the observation port concentrations (c_{Raff}, c_{Extr}, and c_{Rcyl}) can be obtained. To estimate the model parameters and to search the optimal future operating conditions, the simplified process model should be able to compute timely. In this work, the 8-core PC (Intel i7, Windows 7) was used for the simplified process model computation. For binary separation case (c_{Feed} = 1.0 g/L, 1.0 g/L), it took less than 0.6 millisecond for one switching interval simulation (at the same condition, a rigorous process simulator took about 40 seconds), so that the parameter estimation and future prediction were done at each switching interval (The fixed port switching interval is one minute.).

In Fig. 5, the concentration profiles of the rigorous process model and the simplified process model were compared. From the *feed* port, the *extract* port is located at -10 cm, and the *raffinate* port is located at 10 cm. Both ends (20 cm and -20 cm) are located at the *desorbent* port. The observation of *desorbent* port provides the baseline concentrations that should be maintained at zero in well-posed profiles, and the observation of both product streams provide if the mixture is well separated in the zones 2 and 3. Therefore, the simplified process model can properly mimic the real process behavior with three observation ports. In pseudo-binary case, there are two waste components. Since at least one side of the elution profile of waste component is not observed in the observation ports (component B at the desorbent port and component C ant the extract port), it was assumed that the retention factors and cell volumes in the adsorption and desorption sections of the waste components are the same.

4.2 Binary Separation

In the binary separation case (components A and B), the component A (Table 3) is more retained, so that the separated components A and B will be collected at the extract and raffinate ports, respectively. The component A at the extract stream was chosen as a target.

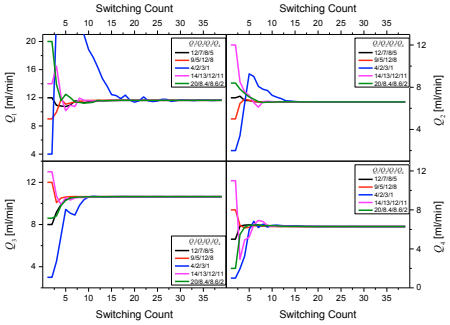

Fig. 6. Comparisons of the controlled zone flow-rate trajectories with different starting points. (c_{Feed} = 0.01 g/L, 0.01 g/L; P = 0.99, Y = 0.99, SC_O = 4, SC_D = 0, SC_F = 4, full information)

To validate the performance of the proposed controller, the controlled trajectories of four zone flow-rates with different initial operating conditions were compared (Fig. 6). If the initial operating conditions are far away from the optimum and the screening algorithm finds a local optimum point (e.g. Nelder-Mead algorithm), the controller could lead wrong operating conditions. To avoid this circumstance, the retention factors estimated at last control cycle were used to

guess the good initial points for the future operation screening (refer to (4)), so that all zone flow-rates were conversed to one optimum conditions in wide range of initial conditions. As the initial conditions are far away from the optimum (e.g. $Q_1/Q_2/Q_3/Q_4$ = 4/2/3/1, blue lines in Fig. 6), it requires longer operations to be converged the optimum. It means that a preliminary short-cut design step (e.g. the triangle method) is still necessary.

Since the process model takes different retention factors and cell volumes in the adsorption and the desorption sections, it is expected that this model can cover the nonlinear retention behaviors.

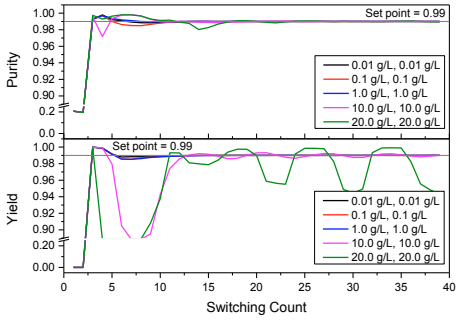

Fig. 7. Comparisons of the controlled purity and yield histories with different feed concentrations. (P = 0.99, Y = 0.99,M = 4, SC_D = 0, SC_F = 4)

Fig. 7 shows the controlled target purity and yield with various feed concentrations in the binary separation case. As the feed concentrations increase, the retention behaviors tend to be nonlinear and competitive.

$$k_i(\vec{c}) = \frac{1-\varepsilon}{\varepsilon}\frac{q_i}{c_i} = \frac{1-\varepsilon}{\varepsilon}\frac{q_{Max}K_i}{1+\sum_{j=1}^{N}K_j c_j} \quad (8)$$

For example, the retention factors of the components A and B are 9.0 and 5.0 in dilute concentration, respectively. However, it is respectively decreased to 7.0 and 3.9 due to the isotherm nonlinearity when the concentrations are each 10 g/L. Therefore, the stability of the controller reduces as the feed concentrations increase. In this case, the maximum controllable feed concentrations are 10.0 g/L each.

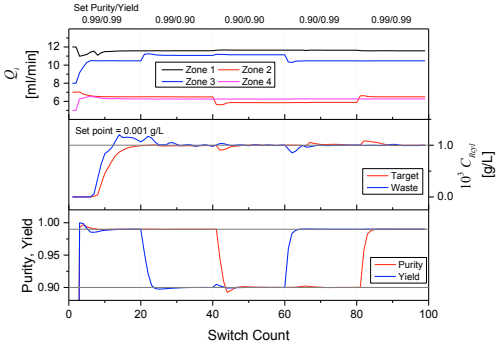

Fig. 8. Controlled zone flow-rate trajectories and process output histories for the binary separation case. (c_{Feed} = 1.0 g/L each, SC_O = 4, SC_D = 0, SC_F = 4, full information)

Fig. 8 shows the control histories for the binary separation case. In every 20 switches, the set purity or yield is changed. The controller starts at the end of the second switching interval. In five switching interval, the controller finds good operating conditions, and all process outputs were converged to the set value with small overshoot. While the flow-rates in the zones 1 and 4 were decided to maintain the desorbent port concentrations, the flow-rates in the zones 2 and 3 were decided to satisfy the set purity and yield. When a new set point is assigned, the controller finds new optimal flow-rates and can remarkably handle the process owing to the precise simplified process model.

4.3 Pseudo-Binary Separation

In the pseudo-binary separation case, one more component (component C, Table 3) was added, and it was chosen as a target. Therefore, the target component C should be collected at the raffinate stream, and rest components (A and B) should be collected at the extract stream.

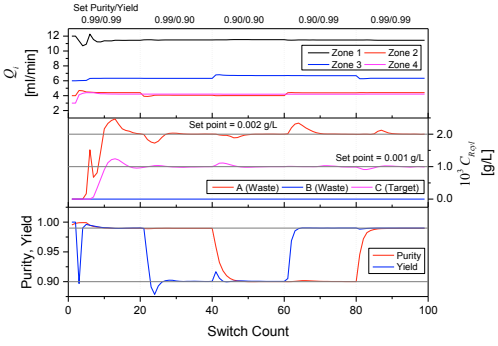

Fig. 9. Controlled zone flow-rate trajectories and process output histories for the pseudo-binary separation case. (c_{Feed} = 1.0 g/L each, SC_O = 4, SC_D = 0, SC_F = 4, full information)

Fig. 9 shows the control histories for the pseudo-binary separation case with the same disturbances in Fig. 8. As the set waste concentration at the desorbent port, $C_{W,Rcyl}$ is decided from the total waste concentration in the feed mixture, it was set to 0.002 g/L. Since the adsorption and desorption parameters of the waste components are the same, bigger overshoot was observed compared to the binary separation case (Fig. 8).

4.4 Control Robustness

In real SMB operation, there are many unexpected factors that affect the separation performances, e.g. experimental measurement error, delayed or incomplete feedback, and system void volumes. With regard to three scenarios (delayed feedback, void volumes, and random error of measurement), the robustness of the controller was investigated.

Since this controller takes the average concentrations of the collected effluents obtained from the chosen analysis method, the delay of feedback information is unavoidable. Therefore, the stability of the controller with delayed information is important for this SMB process.

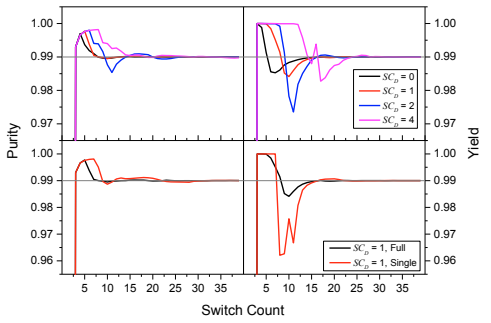

Fig. 10. Comparisons of the target purity and yield histories with different delay scenarios (upper: delay switch counts, lower: Full and Single; the same conditions with Fig. 8)

Fig. 10 compares the controlled target purity and yield histories with different delay scenarios. In delayed or incomplete feedback information, the controller starts with delay and uses past information to estimate the process state. Therefore, the controller finds the optimum with slow convergence. In the investigated delay scenarios, the controller shows good stability. Therefore, the controller allows choosing a good analysis method that requires a certain time, e.g. high-performance liquid chromatography (HPLC).

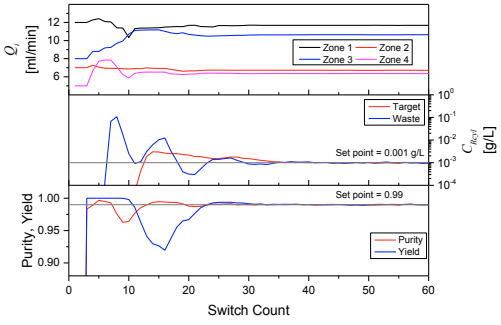

Fig. 11. Controlled zone flow-rate trajectories and process output histories for the binary separation case. (the same initial conditions with Fig. 8, SC_O = 8, SC_D = 1, SC_F = 4, V_{CF} = 0.5 ml, V_{CR} = 0.5 ml, V_{Feed} = 1.0 ml, V_{Extr} = 5.0 ml, V_{Raff} = 5.0 ml, V_{Rcyl} = 5.0 ml)

For a pseudo-real process control, two different types of system void volumes were considered (Table 1). Compared to the empty column volume (7.85 ml), moderate void volumes were chosen (V_{CF} = 0.5 ml, V_{CR} = 0.5 ml, V_{Feed} = 1.0 ml, V_{Extr} = 5.0 ml, V_{Raff} = 5.0 ml, V_{Rcyl} = 5.0 ml). To mimic the fluctuation of experimental measurement, a random number between 0.95 and 1.05 was multiplied to the feedback information. To increase the controller stability for this rough condition, the observation and future prediction switch counts were increased to 8.

Fig. 11 shows the control histories for the binary separation case with the same initial conditions as in Fig. 8. Since, the simplified process model does not consider any system void volume and feedback error, the controller cannot estimate correct process states at the beginning. Therefore, the controller requires quite long switch counts to estimate process states correctly. After 24 switch counts (6 complete cycles), the zone flow-rates were converged to the optimum and all control variables were well maintained to the set points over 36 switch counts (9 complete cycles).

5. CONCLUSIONS

In this work, the authors introduced the frame of the model predictive control method using a novel simplified process model that uses a few meaningful parameters (the retention factor and the cell volume) to control the four-zone SMB process. The process model with linear isotherms can represent the retention behaviors in moderate nonlinear ranges of the competitive Langmuir isotherms. Owing to the simplified process model, the four-zone SMB process can be controlled for chosen binary and pseudo-binary separation cases. The controller can tolerate unconsidered system void volumes and experimental measurement errors including delayed and incomplete feedback information.

REFERENCES

Bentley, J., Kawajiri, Y. (2013) Prediction-Correction Method for Optimization of Simulated Moving Bed Chromatography. AIChE J., 59, 736.

Broughton, D.B., Neuzil, R. W., Pharis, J. M., Brearley, C. S. (1970). The parex process for recovering paraxylene. *Chem. Eng. Prog.*, 66, 70.

Chung, C.F., Wen, C.Y. (1968). Longitudinal dispersion of liquid flowing through fixed and fluidized beds. *AIChE J.*, 14, 857.

Grossmann, C., Langel, C, Mazzotti, M., Morbidelli, M., Morari, M. (2010a). Multi-rate optimizing control of simulated moving beds. *J. Process Control*, 20, 490.

Grossmann, C., Langel, C, Mazzotti, M., Morari, M., Morbidelli, M. (2010b). Experimental implementation of automatic 'cycle to cycle' control to a nonlinear chiral simulated moving bed separation. *J. Chromatogr. A.*, 1217, 2013.

Lee, D., Wiswall, M. (2007). A parallel implementation of the simplex function minimization routine. *Comput. Econ.*, 30, 171.

Natarajan, S., Lee, J.H. (2000). Repetitive model predictive control applied to a simulated moving bed chromatography system. *Comput. Chem. Eng.*, 24, 1127.

Schramm, H., Grüner, S., Kienle, A. (2003). Optimal operation of simulated moving bed chromatographic processes by means of simple feedback control. *J. Chromatogr. A*, 1006, 3.

Storti, G., Mazzotti, M., Morbidelli, M., Carra, S. (1993). Robust design of binary countercurrent adsorption separation processes. *AIChE J.*, 39, 471.

Toumi A., Engell S. (2004). Optimization-based control of a reactive simulated moving bed process for glucose isomerization. *Chem. Eng. Sci.*, 59, 3777.

Toumi A., Engell S., Diehl M., Bock H.G., Schlöder J. (2007). Efficient optimization of simulated moving bed processes. *Chem. Eng. Process.*, 46, 1067.

Vilas, C., Wouwer, A.V. (2011). Combination of multi-model predictive control and the wave theory for the control of simulated moving bed plants. *Chem. Eng Sci.*, 66, 632.